

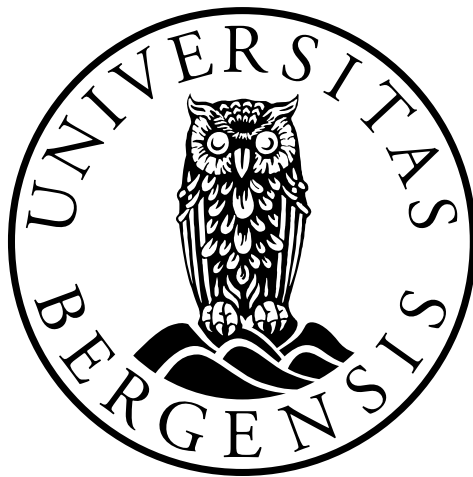
The Medipix ASIC is useless for my project

by

Øyvind Lye

THESIS
for the degree of
MASTER OF SCIENCE IN PHYSICS

(Specialisation in Microelectronics)



Department of Physics and Technology
University of Bergen

September 2016

Contents

1	Introduction	1
1.1	Background and motivation	1
1.2	Goal of the thesis	1
1.3	Structure of the thesis	1
1.3.1	Citations	2
1.4	Scientific environment	2
2	Theory	3
2.1	Radiation	3
2.1.1	Interactions of radiation with matter	3
Interactions of charged particles with matter	3	
Interactions of photons with matter	4	
2.1.2	Biological effects of radiation	5
2.2	Radiation therapy	7
2.2.1	Proton therapy	8
2.3	Radiation detectors	11
2.3.1	Semiconductor detectors	12
2.4	Detector readout	12
2.4.1	Pre-amplifier	13
Charge-Sensitive Amplifier Operation	13	
2.4.2	Shaper	14
2.4.3	Analog-to-Digital Conversion	14
2.4.4	Digital Signal Processing	15
2.5	Semiconductor Characterization	15
2.5.1	Capacitance-Voltage measurements	15
2.5.2	Current-Voltage measurements	16
3	Testing and Characterization of the 3DMiMic Detector	17
3.1	3DMiMic	17
3.2	I-V Measurements of 3DMiMic Detectors	19
3.3	Detector Interface PCB	19
4	Choice of Readout Electronics for the 3DMiMic Detector	20
4.1	Medipix and Timepix	20

4.2	UiO Portable Front-End Readout System	20
4.3	IDEAS Amadeus preamp-shaper	20
4.4	Ortec 142A pre-amplifier	21
4.5	Portable PCIe ADC System	21
	Bibliography	22
	Glossary	24
	Appendices	25
A	3DMiMic Layouts	26
B	Detector Interface PCB	29

Chapter 1: Introduction

1.1 Background and motivation

In 2013 the Norwegian government started a project to build centers for cancer treatment using proton radiotherapy. The main reason for this is that radiotherapy using protons does less damage to healthy tissue than the more conventional radiotherapy using photons that Norway has today. Many photon radiotherapy patients develops cancer again a few decades after the original treatment as a result of the treatment radiation, which makes photon radiotherapy little suited for treating cancer in children. Every year 1000 to 1500 Norwegians will experience fewer side effects by being treated with protons instead of photons [Lynnebakken, 2012]. When treating cancer with protons it is critical to be able to deposit the energy of the radiation at the correct position inside the patient, both to kill the tumor and to avoid unnecessary damage to healthy tissue around the tumor. More on this in section 2.2.1.

To be able to assure the quality of the treatment system, the hospitals need to be able to predict how the energy from a beam of protons will be absorbed in the body. The uncertainties because of the lack of knowledge on this causes an increased risk of side effects for proton therapy patients. To bolster the research on the effects of radiation on humans, SINTEF is developing a silicon based radiation detector (see section 2.3), named Si-3DMiMic, which mimics the response of biological tissue to ionizing radiation on a cellular and sub-cellular level. By measuring how the energy is distributed in the detector, researchers will learn more about how a patient will react to the same radiation beam. [SINTEF, 2015]

1.2 Goal of the thesis

1.3 Structure of the thesis

Chapter 1: Introduction

Introduces the thesis, including background, motivation and goals.

Chapter 2: Theory

Important theory for full understanding of the thesis. Includes theory of radiation,

radiation detection, radiotherapy

1.3.1 Citations

Citations in this thesis generally follows the guidelines recommended for Wikipedia authors. A citation placed after the last punctuation in a paragraph supports multiple claims through the paragraph, while a citation placed before a punctuation only supports one or a few claims just before the citation. In this thesis, citations at the end of a paragraph is much used in the theory sections, where they refer to sources with more detailed information for the interested reader.

1.4 Scientific environment

This master project is supervised by Professor Kjetil Ullaland in the electronics and measurement science research group at the Department of Physics and Technology (IFT) at the University of Bergen (UiB). The 3DMiMic project is a part of the subatomic physics research group at IFT and this master project was assigned by Professor Dieter Röhrich of this group. The Ph.D. dissertation of Röhrich's student Andreas Tefre Samnøy shares many of this master projects objectives. Post doctor Kristian Smeland Ytre-Haugen at IFT leads an ongoing project that looks into microdosimetry and relative biological effectiveness of proton and heavy ion therapy.

SINTEF's department of Microsystems and Nanotechnology produces the 3DMiMic pixel detector that this project is based on. The University of Oslo (UiO) and the University of Wollongong (UOW) is also involved in the 3DMiMic project.

Haukeland?

Chapter 2: Theory

2.1 Radiation

Radiation is defined as the emission and propagation of energy through space or a material medium. Previously radiation was split into groups depending on if it was transferred through particles or waves. This was changed after 1924 when Louis de Broglie claimed that all matter has a wave-like nature. Now, *particle radiation* refers to energy propagated by particles with a definite rest mass and within limits at any instant have a definite momentum and defined position. A particle beam is a group of particles that move in the same direction, similar to a light beam. Examples of these particles are electrons, neutrons, protons, and heavy ions. *Electromagnetic radiation* is energy propagated by the massless photons in phenomena such as light waves, radio waves, microwaves, X-rays, and gamma (γ) rays. Electromagnetic waves propagate at the speed of light and are represented by the spatial intensity variations of an electric field and a magnetic field. [Khan and Gibbons, 2014, chap. 1]

Ionizing radiation carries enough energy to break molecular bonds by *ionizing* atoms it passes, meaning that the atom acquires a positive or negative charge. If the radiation strips an electron from the atom, it becomes a positive ion. If a stripped electron later combines with a neutral atom, it becomes a positive ion. Charged particles with enough kinetic energy is called *directly ionizing radiation* because they can ionize atoms through collisions. Uncharged particles are known as *indirectly ionizing radiation* as they *excite* atoms, raising electrons to higher energy levels. An excited atom can later emit directly ionizing radiation through an electron. [Khan and Gibbons, 2014, chap. 5] See section 2.1.1 for more on this.

2.1.1 Interactions of radiation with matter

Interactions of charged particles with matter

Charged particles, for example protons, primarily react by ionization and excitation. Electrons also commonly react through bremsstrahlung (deceleration radiation), where the particle is decelerated and emits the lost kinetic energy as a photon. When charged particles travel through a medium, they interact with atomic electrons and

nuclei through the Coulomb force. These interactions can be inelastic collisions with atomic electrons, or elastic scattering without energy loss. In the inelastic collisions, the particle loses part of its kinetic energy to produce ionizations and excitations of atoms. This results in energy being absorbed in the medium as the particle is decelerated. [Khan and Gibbons, 2014, chap. 5 & 27]

Stopping power is the average rate of energy loss of a particle per unit path length ($-dE/dx$) in a medium. The Linear Energy Transfer (LET) of a particle is the energy locally deposited per length and is usually expressed in MeV/cm or $\text{keV}/\mu\text{m}$. The LET will always be equal to or smaller than the stopping power. These parameters are used to describe energy deposition in matter and the biological effect of radiation (see section 2.1.2). The LET of a heavy charged particle (a particle of equal or greater mass than a proton) travelling through matter is inversely proportional to the square of its velocity. This means that as the particle loses energy and slows down, the rate of energy loss will increase and the particle slows down at a faster rate. The rate of energy loss (and energy deposition in the medium) becomes maximum as the particle velocity approaches zero. This leads to the particle stopping relatively quickly after travelling a certain distance and makes it possible to define a range for a certain type of particle with a defined energy in a type of matter. The intensity of a particle beam plotted versus depth in tissue can be seen in figure 2.1 where the sudden drop in the proton plots is defined as the particle's range for that energy. [Khan and Gibbons, 2014, chap. 27]

Interactions of photons with matter

The five dominating processes for photon interactions with matter are Rayleigh scattering, the photoelectric effect, the Compton effect, pair production, and photodisintegration. Rayleigh scattering happens when a low energy photon collides with an electron and is scattered to a different angle. This does not deposit any energy in the medium, but the photon is scattered away from its original path. The photoelectric effect is a phenomenon where all the energy of a photon is absorbed in an atom. This leads to one of the orbital electrons being kicked out, and the shell vacancy will lead to emission of X-rays as a higher energy electron fills the vacancy. Occasionally, these X-rays will also kick out more electrons. The Compton effect is when a photon kicks out an electron from an atom and is scattered with reduced energy. The photons lost energy is given to the electron as kinetic energy. Pair production can happen with photons of energy greater than 1.02 MeV, where a photon travelling near an atomic nucleus gives all its energy to produce an electron and a positron. The positron will

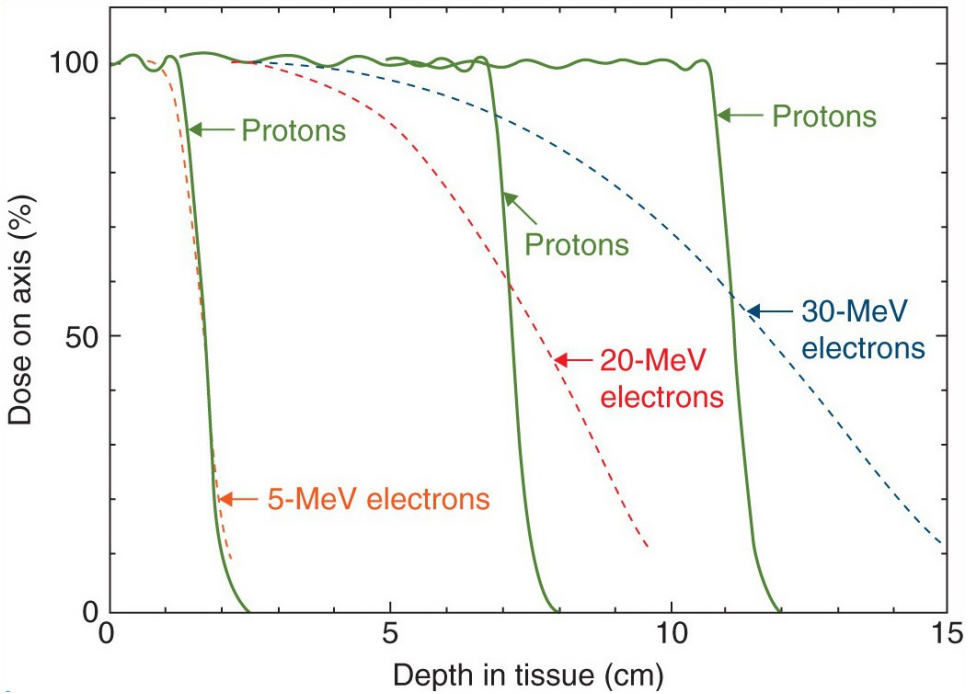


Figure 2.1: Comparison of depth dose distribution for protons and electrons of different energies. [Khan and Gibbons, 2014, fig. 5.15]

later find an atomic electron and they will annihilate each other by producing two photons of 0.51 MeV each. A high energy photon can cause photodisintegration by reacting with an atomic nucleus, leading to a nuclear reaction. [Khan and Gibbons, 2014, chap. 2 & 5]

Due to all the above processes, a photon travelling through matter will at each instant in time have a certain chance of being absorbed in or scattered by the medium. Because of this, the intensity of a photon beam will start to go down instantly when it leaves vacuum, but will take a very long time to be reduced to zero, see figure 2.2. It is therefore impossible to define the range of a photon beam, as is possible with a beam of heavy charged particles. The reduction in the number of photons is proportional to the number of incident photons through the *attenuation coefficient*. [Khan and Gibbons, 2014, chap. 5]

2.1.2 Biological effects of radiation

As discussed in the previous sections, radiation travelling through matter deposits energy in the medium. Examining the effects of this in biological tissue is an extremely complex field. Non-ionizing radiation can heat the matter it passes through, which might cause damage such as sunburns. Ionizing radiation is much more dangerous

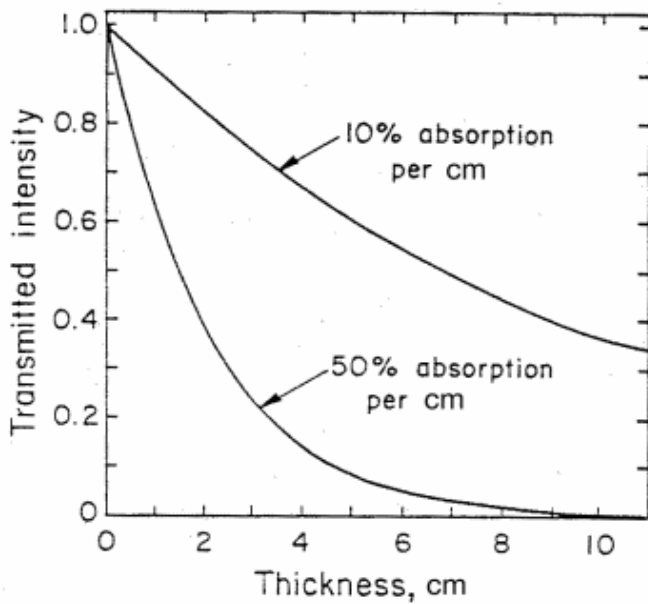


Figure 2.2: Photon intensity through an absorber as a function of thickness [ASU, 2000]

as it breaks molecular bonds, causing molecules to fall apart. This can cause massive damage to tissue cells, change the genetic material (DNA), and destroy the components that produce red blood cells. [Young et al., 2007, chap. 43]

When a cell has been damaged by radiation, there are three possible effects: The cell dies, the cell is repaired correctly, or the cell is repaired incorrectly. The human body has very effective repair mechanisms which constantly repair cellular damage, including damage to DNA. Occasionally, these repair mechanisms will perform their function incorrectly, which can result in cells that cannot perform their normal function, or cells that damage other cells. Some of these cells are unable to reproduce themselves, while others reproduced at an uncontrolled rate, which can be the cause of cancers.[JLab]

To be able to describe the quantity of ionizing radiation for all energies, materials, and types of radiation, it is common to use the quantity *absorbed dose*, or simply *dose*, which is a measure of the biologically significant effects that ionizing radiation produces. It is defined as the energy delivered to tissue per unit mass. The SI unit for dose is gray (Gy), where $1\text{Gy} = 1\text{J/kg}$. The quantity *dose equivalent* has been defined because the biological effects of radiation depend on the type of radiation in addition to the dose. Dose equivalent is the dose multiplied by a quality factor for the type of radiation, in units of sievert (Sv). $1\text{Sv} = 1\text{J/kg}$. Additionally, the sensitivity to radiation-induced effects will vary for different types of tissue, leading to the definition of *effective dose*

equivalent, defined as "the sum of the weighted dose equivalents for irradiated tissues or organs". [Khan and Gibbons, 2014, chap. 8 & 16]

2.2 Radiation therapy

Radiation therapy, also known as radiotherapy, is therapy using the biological effects of ionizing radiation to kill or control cancer cells. One of the main principles behind radiotherapy's effectiveness in treating cancer is that radiation causes much more damage to rapidly dividing cells, and tumor cells divide extremely rapidly [Serway and Jewett, 2014, chap. 45]. Roughly half of all cancer patients receive radiotherapy as a part of their treatment. The radiation can originate from a machine outside the body (external beam radiation therapy), or from a radioactive source being placed into the body (internal radiation therapy). Traditional external beam radiation therapy is delivered using photon beams (photon therapy), but treatment with beams of heavy charged particles (particle therapy), like protons (proton therapy) or carbon ions, are becoming more common. Electron beam therapy is also used, mainly to treat cancer close to the surface of the body. [NIH, 2010]

The radiation will also damage healthy tissue, but a lot of work is put into reducing this as much as possible. Planning and simulations are done to increase the certainty of avoiding complications. Detailed imaging scans are done to get a 3D map of the patient's tumor and surrounding areas. The basis for these maps are usually Computed Tomography (CT) scans, but can also be combined with Magnetic Resonance Imaging (MRI), Positron Emission Tomography (PET), X-ray images, or ultrasound scans [NIH, 2010]. One of the main reasons for CT's importance for photon therapy is that as it is based on photon beams, a CT scan also yields the body's tissue-density information and photon attenuation coefficient, which is needed for photon therapy planning. [Khan and Gibbons, 2014, chap. 12]

The particle beams of external beam radiation therapy are of high energy and needs to be produced in or near the treatment machine. For photon therapy, it is most common to accelerate photons using a linear accelerator (linac), which is small enough to fit inside the same room as the patient table [NIH, 2010]. For particle therapy a bigger and more expensive accelerator is needed to accelerate the particles to high enough energies. For proton therapy a cyclotron or a synchrotron is used. [Khan and Gibbons, 2014, chap. 27]

The dose is usually delivered once per day every workday for 4-6 weeks. One de-

livery is called a fraction. Fractionation is done for multiple reasons: One is to allow healthy tissue time to repair the damage from radiation. Another is to increase the chance of hitting the cancer cells at a time when they are vulnerable. Fractionation also helps to minimize the effects of random variations in the patient's position and internal geometry. [Board of the Faculty of Clinical Radiology, 2006] [Hysing, 2015]

As already mentioned, radiation therapy also damages healthy tissue, which can produce both acute (early) and chronic (late) side effects. Acute side effects occur before the treatment ends, and is usually temporary. Examples include skin irritation, hair loss, fatigue and nausea. Chronic side effects develop months to decades after treatment is complete. Examples are skin damage, memory loss, infertility and second cancer. Second cancer is the development of a new cancer in a person that has previously had cancer. As this takes a long time to develop, it might not be a very large problem for older patients, but it is critical to avoid second cancer when treating cancer in children and adolescents. [NIH, 2010]

When plotting the absorbed dose in water (or tissue), the differences between photon beams and heavy charged particle beams become even more apparent than when plotting the intensities (section 2.1.1). Figure 2.3 shows the relative dose deposited in water for a proton and a photon beam. The photon beam's maximum is very close to the surface, and the photons will damage tissue far into the body. Also, if the tumor is deep into the body, and the beam only comes from one direction, the photons will have to do a lot of damage to the skin to be able to do enough damage to the tumor. Protons (and other heavy charged particles) on the other hand have their maximum deeper into the material, in what is called the *Bragg peak*. Protons deposit less energy before the maximum, and close to no damage behind the maximum.

2.2.1 Proton therapy

Proton therapy is radiation therapy using high energy proton beams. The main principle behind the use of proton therapy is to exploit the Bragg peak to deposit a high dose to a tumor, with low dose delivered in front of it, and close to no dose behind. The Bragg peak is very narrow and is not able to cover most tumors, which has lead to the use of superposition of multiple beams of different energies. This superposition is called a Spread-Out Bragg Peak (SOBP), see figure 2.4. A SOBP has a lot higher dose deposited in front of the tumor than a single proton beam, but it is still lower than that of a photon beam. The dose behind the tumor is still low. [Khan and Gibbons, 2014, chap. 27]

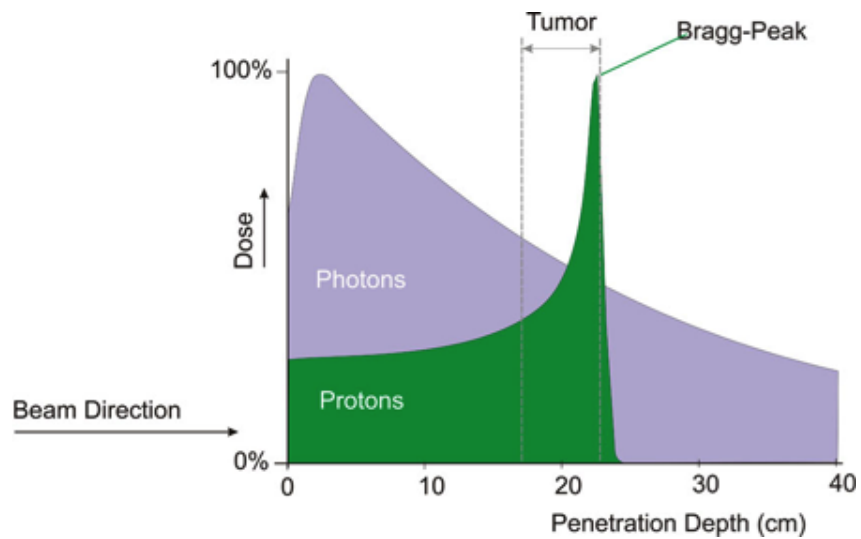


Figure 2.3: Percentage depth dose for a photon beam and a proton beam in tissue. [P-Cure]

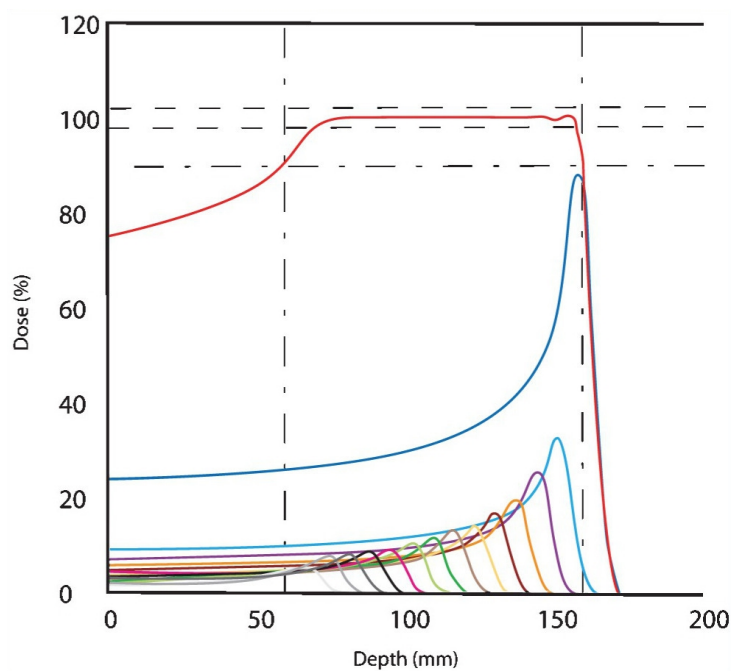


Figure 2.4: SOBP depth dose distribution [Khan and Gibbons, 2014, fig. 27.10]

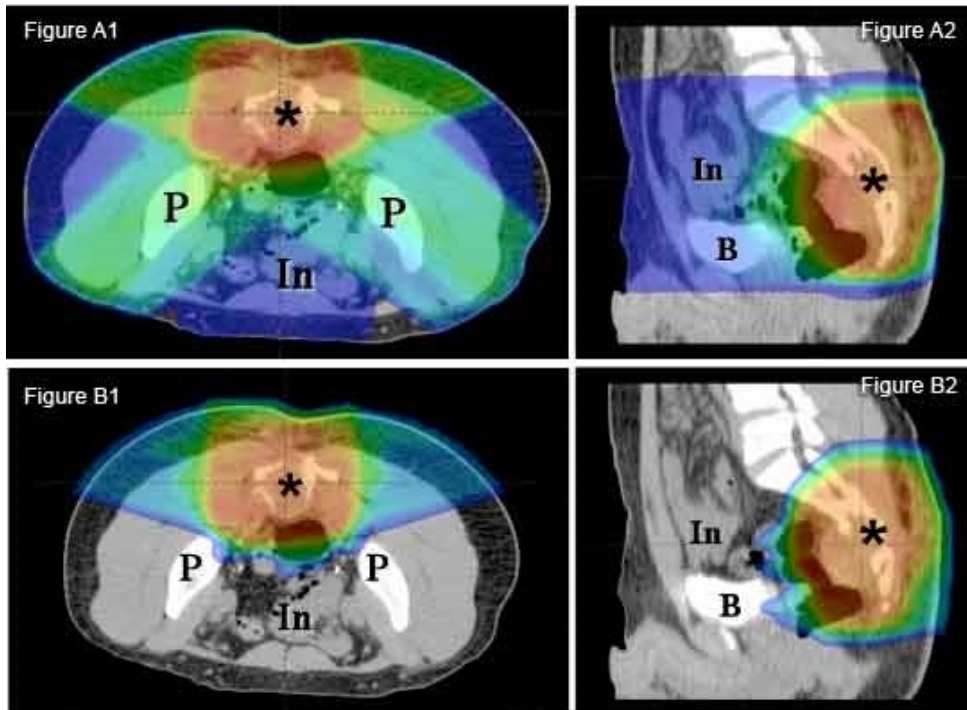


Figure 2.5: Photon (A1 & A2) and proton (B1 & B2) beam dose distributions. [P-Cure]

The shape of the SOBP makes it possible to treat tumors with a lot less dose to the surrounding tissue than with photon therapy, which has two main benefits. One is the ability to treat tumors in close proximity to critical organs without damaging said organ. The other is to avoid the chronic side effects mentioned in section 2.2, which is very important when treating children with cancer [Khan and Gibbons, 2014, chap. 27]. Figure 2.5 compares photon (A) and proton (B) beams, where red is high dose, blue is low dose, and gray is negligible dose.

The geometrical accuracy in proton therapy is a lot more critical than in photon therapy. While a geometrical error between planning and delivery in photon therapy will give a smaller under-dosage to the tumor and over-dosage to surrounding tissue, similar errors in proton therapy could cause part of the tumor receiving no dose at all and healthy tissue receiving full dose, see figure 2.6. Geometrical uncertainties can come from setup and anatomical variations, biological considerations, organ motion, and dose calculation approximations. [Paganetti, 2012]

As mentioned in section 2.2, photon CT yields the patient's photon attenuation coefficient that is needed for photon therapy, but for proton therapy the stopping power is needed to greatly reduce range errors. Therefore proton CT imaging techniques are being developed, based on the same principles as conventional CT, but using low-

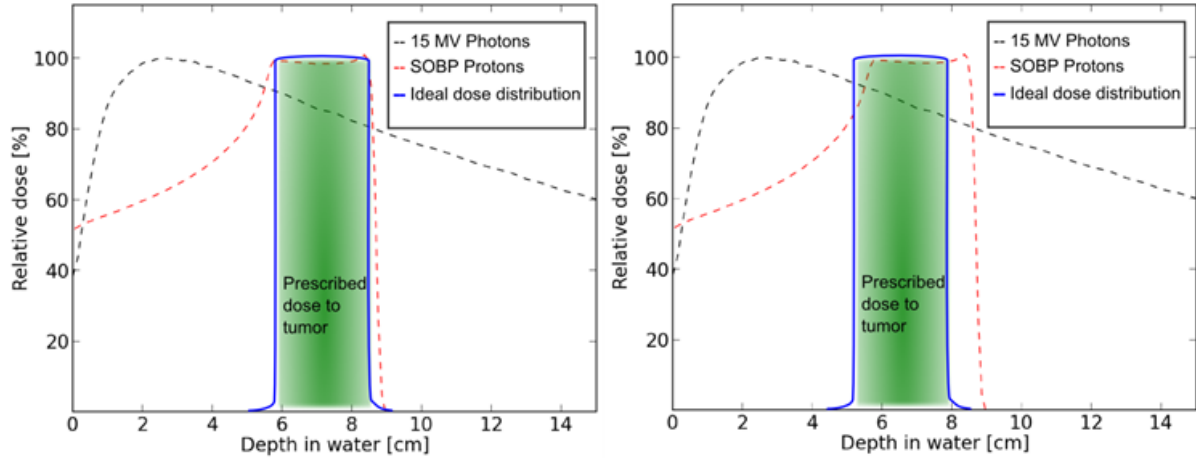


Figure 2.6: Comparison of dose distribution with correct (left) and incorrect (right) range assumptions. [Ytre-Hauge, 2015]

intensity proton beams instead of photon beams. [Freeman, 2013]

Proton therapy can theoretically be delivered in a low fewer fraction than photon therapy due to lower dose to surrounding tissue, but this is very risky in case the target is missed.

2.3 Radiation detectors

A radiation detector records interactions between incoming radiation and the detector. These interactions could be electrical, chemical, light- or heat-based. Detectors can be based on many different materials, including gas chambers, semiconductors, crystals, and liquid. In a simple radiation detector a single particle interacts with the detector, resulting in an electric charge appearing inside the detector. This charge is typically collected by setting up an electric field inside the detector, which causes positive and negative charge to flow in opposite directions, forming an electric signal. This signal could be measured as a current (current mode), voltage (mean square voltage mode), or a charge (pulse mode). [Knoll, 2010, chap. 4]

Pulse mode is the most common readout mode because the measurement records each individual quantum of radiation. Pulse mode is therefore required when attempting to measure the energy of individual radiation events. The charge generated in the detector is usually integrated over a certain period of time. Pulse mode however does not work well at very high event rates as the time between events becomes too short to analyse the data. Current mode measures the average current over many events, therefore loosing the amplitude and timing information of individual events, but al-

lowing for measurement with high event rates. Mean square voltage mode works much like current mode, but the output signal will be more dependent on the charge per event, making this mode more useful for mixed radiation environments. [Knoll, 2010, chap. 4]

2.3.1 Semiconductor detectors

Semiconductor diode detectors, also called simply semiconductor detectors or solid-state detectors, are radiation detectors employing semiconductor diodes as the basic detection medium. Silicon is the most common material used, but germanium detectors are superior for gamma-ray measurements. Semiconductor detectors offer energy resolutions that are superior to other radiation detectors in addition to small size and fast timing characteristics. A big drawback is that they are degraded by radiation-induced damage during normal use. [Knoll, 2010, chap. 11]

Charged particles passing through a semiconductor detector create electron-hole pairs along the particles path. By setting up an electric potential across the diode, there will be an electric field present that will cause the holes to drift in the same direction as the electric field vector, and the electrons in the opposite direction. By monitoring one of the diodes sides, a pulse is measured as the charge from either the holes or the electrons (depending on which side is measured) is collected.

A semiconductor detector, like other diodes, can be forward biased (positive potential on p-side) or reverse biased (positive potential on n-side). It is possible to operate a semiconductor detector without external bias, but it will perform poorly as the electric field across the junction will be too weak to read out the charge carriers before many are lost. Applying forward bias to the detector reduces the electric field even further, while reverse bias increases it. This is the main reason for reverse bias being the dominant choice for radiation detectors. [Knoll, 2010, chap. 11]

2.4 Detector readout

In different situations, the desired output from the detector readout will be different. In some cases, it is enough to simply count the radiation quanta, and in other cases one might want to read out a energy spectrum. In both cases the readout chain starts with a pre-amplifier that produces a voltage that is proportional to the radiation charge. The output from the pre-amplifier is sent to a shaping amplifier which converts the signal to a shape that is more suitable for the next component in the readout chain. This is to select the interesting pulses and convert the analog signal to a digital signal

in one way or another. [Knoll, 2010, chap. 16]

2.4.1 Pre-amplifier

For most radiation detectors, the liberated charge is too small to be processed, which is why pre-amplifiers are needed in most detector readout chains. The pre-amplifier is located close to the detector to reduce noise. A pre-amplifier can be voltage-sensitive or charge-sensitive. A voltage-sensitive pre-amplifier has an output signal proportional to the input voltage, which will be proportional to the input charge if the detector capacitance is constant. This is not the case for semiconductor detectors where the capacitance may change with the operating parameters. A charge-sensitive pre-amplifier (CSA) has a output signal that is independent of the input capacitance as long as the amplifier gain is high enough compared to a relationship between capacitances in the system. [Knoll, 2010, chap. 16]

One often important parameter to consider in a pre-amplifier is the dynamic range, which is the range of input signal amplitudes that can be reliably measured without changing the system. The lowest measurable input signal is limited by the noise in the system, mainly in the detector, detector cables, and pre-amplifier. A signal is not reliable if it is difficult to discern from the noise. The highest measurable input signal can be limited by the pre-amplifier or later stages, like the Analog-to-Digital Converter (ADC). If the pre-amplifier has a high gain, then a large input signal will require a higher output signal than the pre-amplifier can deliver. If the gain is low, then another stage in the system will likely be the bottleneck before the pre-amplifier reaches its highest output level. [Halámek et al., 2001]

It is typically convenient to use the pre-amplifier to supply bias voltage to the detector. When this is done a single cable is used both to provide voltage to the detector and to transfer the signal pulses to the readout system. [Knoll, 2010, chap. 16]

Charge-Sensitive Amplifier Operation

Figure 2.7 shows a general CSA. When a radiation quanta strikes the detector, a pulse of charge Q_s and width t_o is generated. This creates a rising potential on the negative input of the amplifier, which triggers a falling potential on the output of the amplifier. Because of the negative feedback, this will quickly draw the negative input close to zero, making the negative input a point of virtual ground. The feedback currents charge the feedback capacitor, and then the capacitor is slowly discharged when there is no signal on the input. This creates a voltage pulse on the output that slowly falls

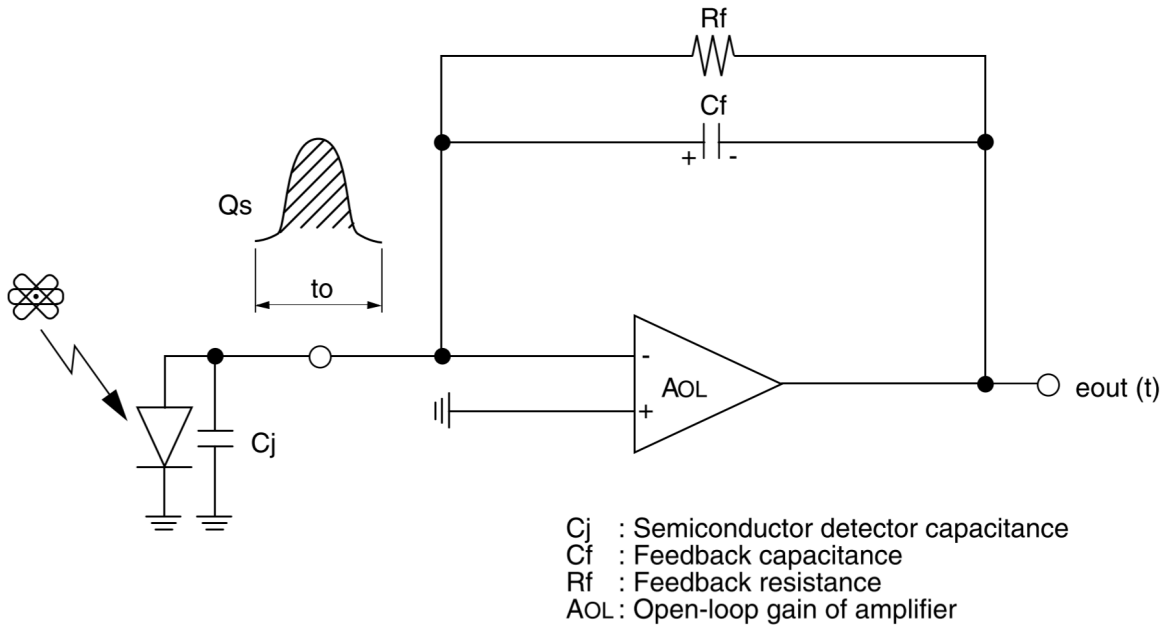


Figure 2.7: Schematic of a basic CSA. [Hamamatsu, 2001]

from a peak value that is proportional to the input charge. [Hamamatsu, 2001]

2.4.2 Shaper

The shaper, or shaping amplifier, converts the shape of the signal to a form that is suitable for measurement. The pulse height of the signal from the shaper is proportional to the input charge. It is important that the output from the shaper quickly returns to the baseline to prevent pulse overlapping that will cause measurement errors. The first stage of the shaper is a differentiator (high pass filter) which passes the steep rise of the input pulse, but quickly returns to the baseline. The differentiator decides the fall time of the pulse. The signal is then amplified to a level that is suitable for the ADC, before it is passed through the integrator (low pass filter) that filters away noise and changes the rise time of the pulse. The duration of the shaped pulse is called the shaping time. [Knoll, 2010, chap. 16]

2.4.3 Analog-to-Digital Conversion

The analog signal from the shaper needs to be converted to a digital signal for processing and storage. When it is desired to keep as much information as possible, an ADC is used, but these use a lot of area and power. In situations where area, power, and cost is more important than accuracy of measurements (typically when there are a lot of channels), there are some simpler methods that can be used instead. The simplest

is a counter, which merely counts the number of pulses with a height above a defined threshold. The information on the radiation quanta energy is lost, but the circuit is very simple. It is also possible to have multiple counters with different thresholds, which will keep some information about the distribution of radiation quanta energies. Another much used method is the Time over Threshold (ToT) technique. A ToT circuit measures the time that the pulse is over a defined threshold, and then this measurement can be used to estimate the height of the pulse. The relationship between pulse height and ToT is only linear within a certain range, and will usually limit the dynamic range of the readout system. [Iniewski, 2010, chap. 6]

An ADC samples the analog signal amplitude at a certain interval (sampling rate) and converts each sampled value to a digital signal. The resolution, which is the number of bits in the digital signal, will limit the accuracy of the conversion. The quantisation error is introduced as each analog value needs to be converted to the closest digital value. The maximum percentage quantisation error can be seen in equation 2.1, where n is the number of digits in the binary code and 2^n is the number of digital values. [Bentley, 2005, chap. 10]

$$e_q^{MAX} = \pm \frac{100}{2(2^n - 1)} \% \quad (2.1)$$

The dynamic range of an ADC will mainly be limited by its resolution, noise, linearity, and jitter (small timing errors).

2.4.4 Digital Signal Processing

2.5 Semiconductor Characterization

2.5.1 Capacitance-Voltage measurements

Capacitance-Voltage (C-V) profiling is a semiconductor characterisation technique that is much used to find doping- and defect densities in semiconductor junctions. The technique relies on the fact that the width of a reverse biased depletion region depends on the applied voltage. The small signal capacitance is dependent on both the doping density and width of the depletion region. C-V profiles are made by measuring the capacitance while sweeping over a voltage range. The doping density is found from the slope of a C-V curve or a $1/C^2$ -V curve. [Schroder, 2005, chap. 2]

There are multiple ways to measure capacitance. A simple method is to supply a

known current, and measure how fast the voltage across the capacitor rises. This method assumes an ideal capacitor, and is therefore inaccurate for a real capacitor. A more accurate method is to supply an AC signal to the Device Under Test (DUT) and measure the AC current and voltage. A high frequency signal (~ 10 MHz) will be better for measuring dynamic performance, while a low frequency signal (~ 10 kHz) is better to find quasistatic characteristics. The capacitance is calculated from the frequency, current, and voltage.

2.5.2 Current-Voltage measurements

Current-Voltage (I-V) characterization is observation of the current through a device when sweeping over the voltage across it. This can be used to find basic electrical parameters for the device. This includes leakage current, resistance, cut-in voltage, breakdown voltage, saturation voltage, and hysteresis.

Chapter 3: Testing and Characterization of the 3DMiMic Detector

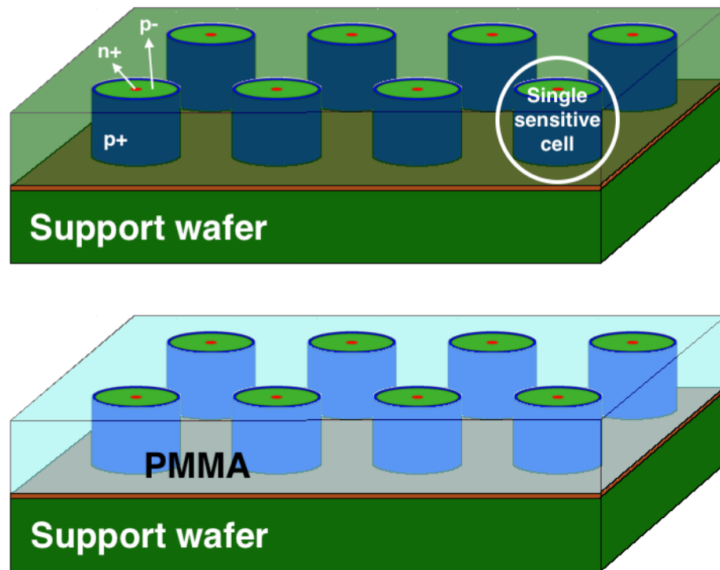


Figure 3.1: Presentation sketches of the 3DMiMic detector, shown without and with polymethyl methacrylate (PMMA). [Povoli et al., 2015]

3.1 3DMiMic

Si-3DMiMic, or simply 3DMiMic, is a silicon-based 3D mini and micro-dosimeter being developed by SINTEF MiNaLab in Oslo, but was invented and ordered by researchers at the University of Wollongong. The detector is made to mimic the response of biological tissues to ionizing radiation on a cellular and sub-cellular level, and consists of an array of 32x32 cylindrical p-i-n diodes. Each diode, or cell, is made of a thin n+ core cylinder (red in figure 3.1), a circular p+ trench some micrometers out (dark blue in figure 3.1), and in some cases a n+ ring further away from the core (to the right in figure 3.2). There are multiple versions of the detectors, with differences including presence of n+ guard ring, size of cell, and structure. The silicon between the different cells should be etched away and replaced with tissue equivalent PMMA, but this has not been attempted by SINTEF yet as of the time this thesis is written. This should be done because PMMA is ionized by radiation very similar to the way tissue would,

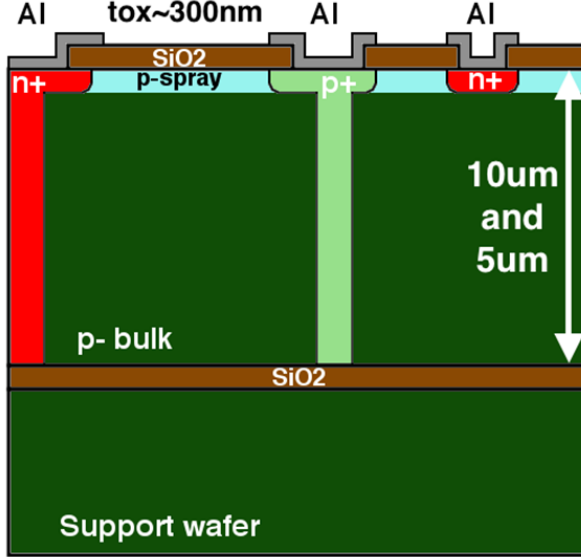


Figure 3.2: Layout of 3DMiMic design with 3D n+ core and 3D p+ trench. [Povoli, 2016]

unlike silicon, due to the mass numbers of the atoms.

Figure 3.2 show a "3D" layout with the n+ core cylinder and the p+ trench going all the way through the bulk, and a planar n+ guard ring. There also exist designs with either or both the n+ core and p+ trench made planar. Figure 3.3 shows the smallest, "15 μm ", layout of 3DMiMic from above with a size scale. The larger, "30 μm ", layout is roughly 25 % larger than the "15 μm " layout. Images of some of the different layouts can be found in Appendix A.

In the main layout of 3DMiMic, all the n+ cores in a line is connected together. Every second line is also connected, leaving two channels (odd/even) for readout. When present, all the outer n+ rings are connected and can be read out if desired. There also exist other layouts, for example with all diodes connected together, readout in eight channels, and a larger design made to be bump bonded to a Medipix chip (see section 4.1).

Even though the odd/even readout scheme contains two channels, it does not provide any spacial information, as both channels cover the whole active area of the detector. The reason for this layout is to notice if a particle track goes through multiple adjacent cells. If both readout channels are triggered at the same time, this was not a single event, as it will look if all cells are read in a single channel.

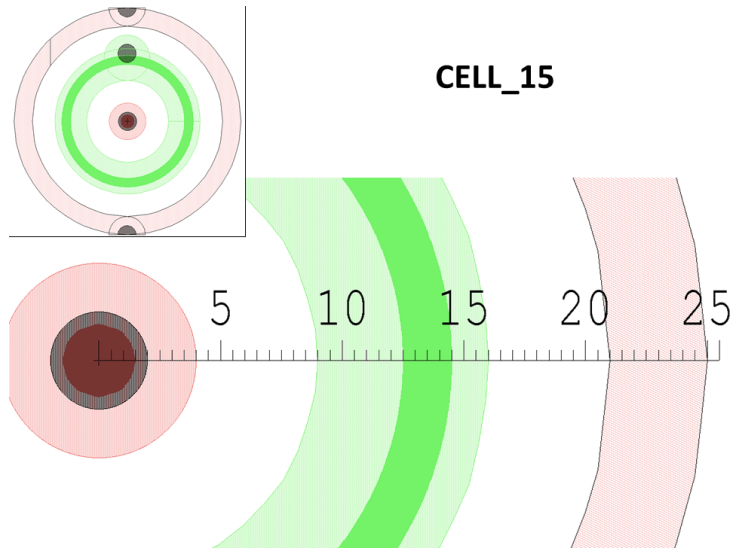


Figure 3.3: Smallest, "15 μm ", layout of 3DMiMic seen from above. Distance scale is in μm . [Povoli, 2016]

3.2 I-V Measurements of 3DMiMic Detectors

I-V measurements of seven 3DMiMic wafers were performed in the cleanroom at SINTEF MiNaLab in Oslo by Øyvind Lye and Andreas Tefre Samnøy in May 2016. These seven wafers have been produced with different designs and fabrication processes. Each wafer has 104 detectors with odd/even readout, 6 detectors with single channel readout, and several other experimental layouts. The detectors had to be tested with manual needle placement, as the designs are too different to use an automatic system with a probe card. The wafer is held in place on a stand using vacuum, and the stand can be moved in the horizontal plane. The needles can be manually placed at the desired location, and the position can be fine-tuned in Cartesian space using screws. The cell n+ guard ring was not connected on the detectors where it is present. This was done because it would require a separate test setup for the detectors with the ring, which would increase the time needed for the measurement. A total of 580 detectors were measured.

3.3 Detector Interface PCB

A Printed Circuit Board (PCB) was designed to interface 3DMiMic to the supply and readout electronics. This is described in more detail in appendix B.

Chapter 4: Choice of Readout Electronics for the 3DMiMic Detector

4.1 Medipix and Timepix

Medipix is a family of chips developed to exploit technology from the experiments at CERN in other fields of science, mainly medical imaging. The chips made by the Medipix collaboration are; Medipix1, Medipix2, Timepix, Medipix3, Timepix3, and Dosepix. The Medipix 1-3 chips are made for photon counting and are therefore not useful for dosimetry. The Timepix chips are made to do ToT measurements, with Timepix and Timepix3 being based on Medipix2 and Medipix3 respectively. Dosepix is a currently in development chip made for photon dosimetry. Timepix3 and Dosepix were considered for the 3DMiMic project, but as ToT devices their dynamic range is not very large. Also, since they are made for photon detectors they cannot read the large charges released by a carbon ion in the Bragg peak.

4.2 UiO Portable Front-End Readout System

During the school year 2014-2015 two master students at UiO made a portable front-end readout system for radiation detectors [Tali, 2015] [Oltedal, 2015]. This system consists of two custom made cards and a Field-Programmable Gate Array (FPGA) evaluation board. The first card, the analog card, has three channels with pre-amplifiers while two of those channels also including shapers. The second card, the digital card, includes an ADC, comparators, and current monitors. The components of the digital card is connected to the FPGA on the SoCKit evaluation board by Arrow, which is connected to a computer through network. The system is made to detect fission fragments which produce very large signals, and therefore has a low gain. This makes the system too noisy for the low noise requirements of the 3DMiMic detector at the default gain, but this can be changed using external components.

4.3 IDEAS Amadeus preamp-shaper

IDE1180, or Amadeus, by Oslo-based IDEAS is an integrated circuit for the front-end readout of radiation detectors. It features 16 channels of CSA and shapers with ad-

justable shaping time. The preliminary datasheet [Maehlum et al., 2015] specifies a shaping time between 20 ns and 40 ns, negative and positive input charges up to 400 fC with lowest gain, and equivalent noise charge of 1106 e- plus 68 e- per pF load at default gain.

This chip was considered by multiple projects at IFT and a evaluation board (7045) was given to IFT so that more extensive tests could be performed.

4.4 Ortec 142A pre-amplifier

Ortec 142A is a single channel low-noise CSA optimized for charged particle or heavy-ion detectors. It was considered for the 3DMiMic project since UiB already owns a few of these. It features a very high dynamic range, but the gain is too low for the 3DMiMic detector.

4.5 Portable PCIe ADC System

The current ADC system used at UiB is a Caen V1729A digitizer sitting in a VMI crate. This features four 14 bit channels with 2 GS/s sampling rate, but is very large and heavy, making it cumbersome to bring for radiation tests. It was desirable to purchase a new ADC for the department that could be put inside a small computer using PCI Express (PCIe) to make a portable system. Three manufacturers that produced suitable ADCs for a reasonable price were found; AlazarTech, Keysight Technologies, and SP Devices. The considered models are listed in table 4.1.

Table 4.1: The analog-to-digital converters considered for purchase.

Manufacturer	Model	Channels	Resolution (bits)	Sampling (GS/s)
AlazarTech	ATS9360	2	12	1.8
Keysight	U5303A	2 (1)	12	1.6 (3.2)
SP Devices	ADQ14AC-2X	2	14	2
SP Devices	ADQ14AC-4C	4	14	1

The Keysight model was interesting with a signal interleaving feature where both 1.6 GS/s channels could be combined into one 3.2 GS/s channel. In the end SP Devices was chosen, being the only discovered company that produces 14 bit PCIe ADCs in the GS/s range. ADQ14AC-4C was chosen as having two extra channels was considered more important than higher sampling rate for radiation tests. The old Caen ADC can be used for projects and tests that require higher sampling rate.

Bibliography

- ASU (2000). Arizona State University: Mechanism for the Absorption of Light. <https://www.asu.edu/courses/phs208/patternsbb/PiN/rdg/mechanism/>. Accessed: 14/10/2015.
- Bentley, J. P. (2005). *Principles of Measurement Systems*. Prentice Hall.
- Board of the Faculty of Clinical Radiology (2006). *Radiotherapy Dose-Fractionation*. Royal College of Radiologists, London.
- Freeman, T. (2013). The potential of proton CT. <http://medicalphysicsweb.org/cws/article/research/53211>. Accessed: 15/10/2015.
- Halámek, J., I. Visčor, and M. Kasal (2001). Dynamic range and acquisition system. *MEASUREMENT SCIENCE REVIEW* 1(1).
- Hamamatsu (2001, 10). *Characteristics and use of Charge amplifier* (KACC9001E01 ed.). Hamamatsu Photonics.
- Hysing, L. B. (2015). Geometrical uncertainties in radiotherapy. Powerpoint presentation from PHYS213 lecture October 2015 at UiB.
- Iniewski, K. (2010). *Electronics for Radiation Detection*. CRC Press.
- JLab. Jefferson Lab: Radiation worker training: Effects of radiation on cells. https://www.jlab.org/div_dept/train/rad_guide/effects.html. Accessed: 06/10/2015.
- Khan, F. M. and J. P. Gibbons (2014). *Khan's The Physics of Radiation Therapy*. Lippincott Williams and Wilkins.
- Knoll, G. F. (2010). *Radiation Detection and Measurement*. Wiley.
- Lynnebakken, H. (2012). Jubler for partikkelterapi. <http://www.mn.uio.no/fysikk/forskning/aktuelt/aktuelle-saker/2012/jubler-for-partikkelterapi.html>. Accessed: 24/09/2015.
- Maehlum, G., D. Meier, and T. Stein (2015, 11). *IDE1180 Preliminary Datasheet* (V1R3 ed.). IDEAS.

- NIH (2010). National Institutes of Health: Radiation Therapy for Cancer. <http://www.cancer.gov/about-cancer/treatment/types/radiation-therapy/radiation-fact-sheet>. Accessed: 09/10/2015.
- Oltedal, E. J. (2015). FPGA based readout of a silicon PIN detector.
- P-Cure. P-Cure Clinics. <http://www.p-cure.com/index.aspx?id=4013>. Accessed: 12/10/2015.
- Paganetti, H. (2012). Range uncertainties in proton therapy and the role of monte carlo simulations. *Physics in Medicine and Biology* 57(11), R99.
- Povoli, M. (2016). From email conversation.
- Povoli, M. et al. (2015). Simulation and testing of thin silicon microdosimeters realized with planar technology. <https://indico.cern.ch/event/351695/contributions/828320/>.
- Schroder, D. K. (2005). *Semiconductor material and device characterization*. Wiley.
- Serway, R. A. and J. W. Jewett (2014). *Physics for Scientists and Engineers with Modern Physics*. Cenage Learning.
- SINTEF (2015). Si-3DMiMic - Silicon-based 3D Mini and Micro-dosimeters. <https://www.sintef.no/en/projects/3dmimic/>. Accessed: 24/09/2015.
- Tali, M. (2015). Portable Front-End Readout System for Radiation Detection.
- Young, H. D., R. A. Freedman, and L. Ford (2007). *University Physics with Modern Physics*. Addison-Wesley.
- Ytre-Hauge, K. S. (2015). Radiation therapy with photons, protons and carbon ions. Powerpoint presentation from PHYS251 lecture march 2015 at UiB.

Glossary

ADC Analog-to-Digital Converter. 13–15, 20, 21

C-V Capacitance-Voltage. 15

CSA charge-sensitive pre-amplifier. 13, 14, 20, 21

CT Computed Tomography. 7, 10

DUT Device Under Test. 16

FPGA Field-Programmable Gate Array. 20

I-V Current-Voltage. 16, 19

IFT Department of Physics and Technology. 2, 21, 29

LET Linear Energy Transfer. 4

linac linear accelerator. 7

MRI Magnetic Resonance Imaging. 7

PCB Printed Circuit Board. 19, 29, 31

PET Positron Emission Tomography. 7

PMMA polymethyl methacrylate. 17

SOBP Spread-Out Bragg Peak. 8–10

ToT Time over Threshold. 15, 20

UiB University of Bergen. 2, 21–23

UiO University of Oslo. 2, 20

UOW University of Wollongong. 2

Appendices

Appendix A: 3DMiMic Layouts

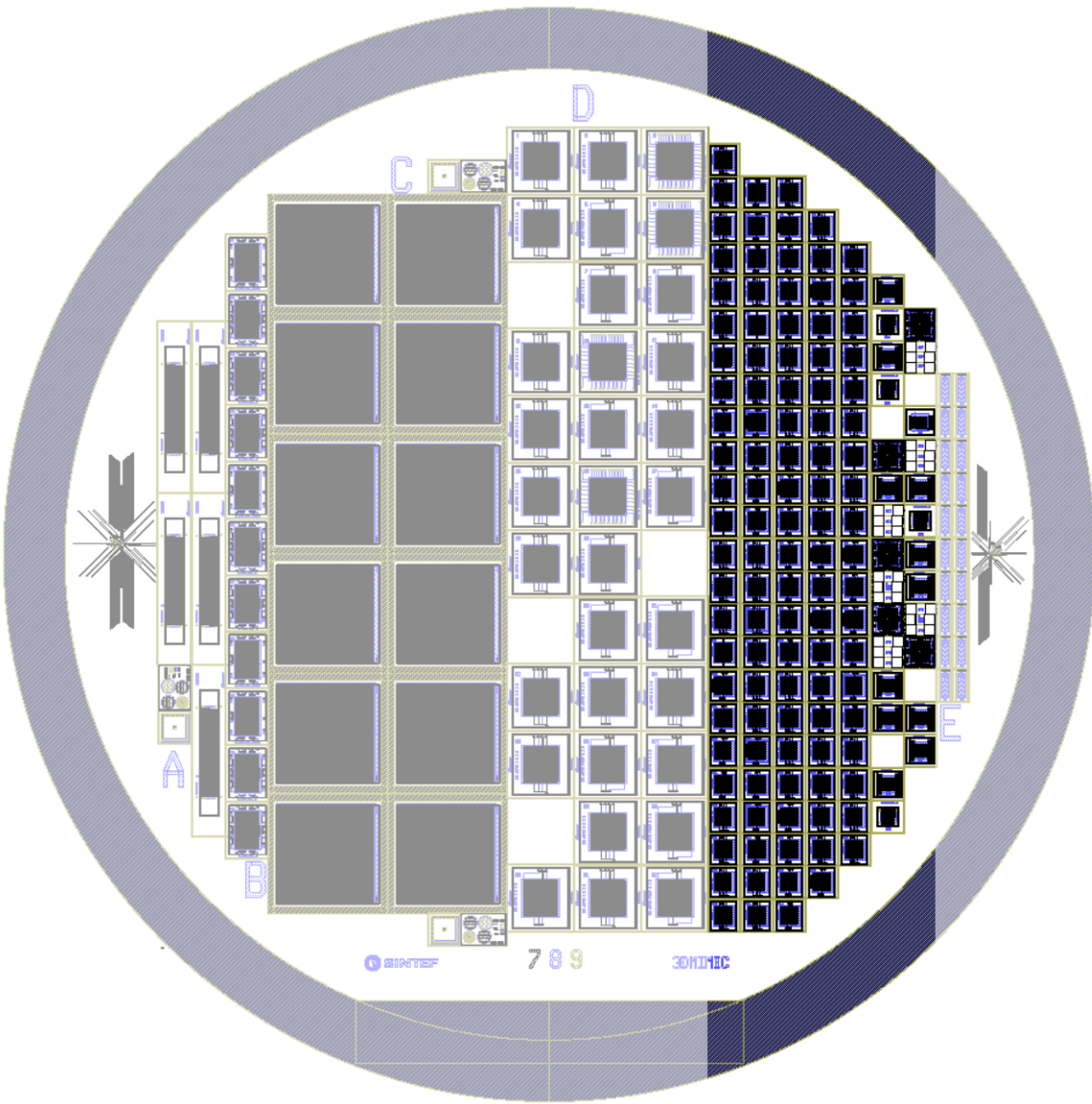


Figure A.1: 3DMiMic wafer.

Figure A.1 shows a whole 3DMiMic wafer. The highlighted area are the detectors that are relevant for this thesis. The large detectors on the left are made to be bump bonded with a Medipix chip. Figures A.3 to A.11 show some of the different layouts in the highlighted area. The detectors with "_L" in the name are of the "30 μm " size, while the others are of the "15 μm " size, see figure A.2. All figures in this appendix are from Marco Povoli at SINTEF.

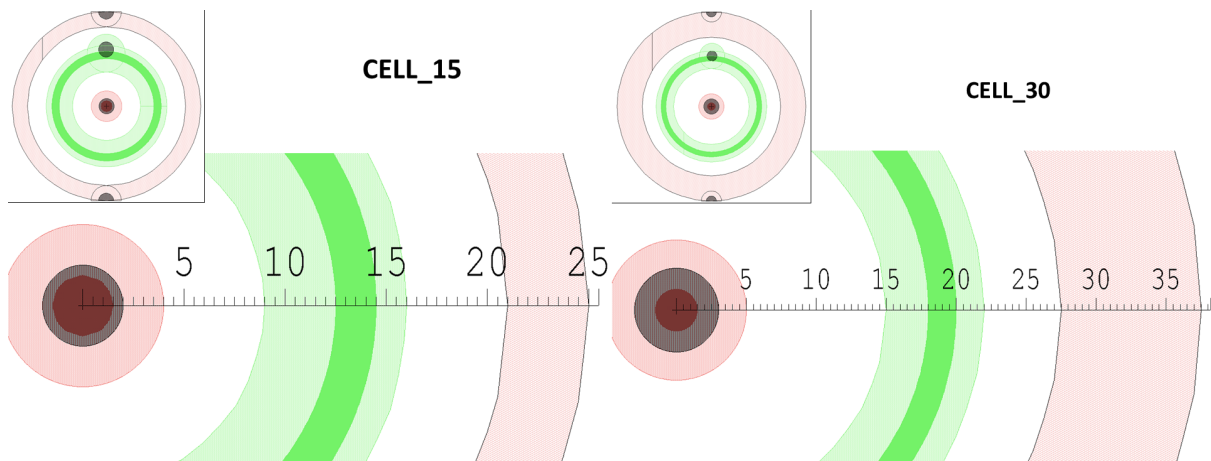


Figure A.2: 3DMiMic cell sizes. Distance scale is in μm .

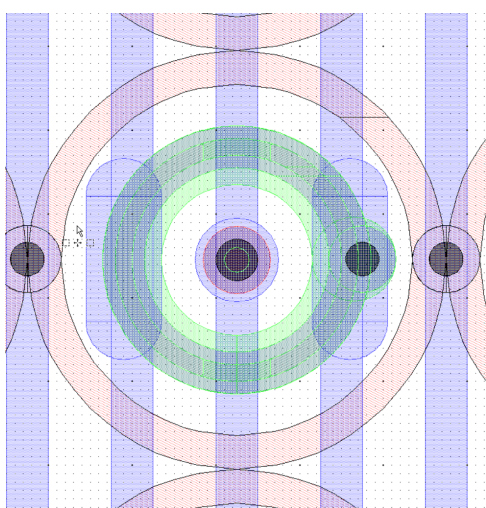


Figure A.3: MIC_ARRAY_1 layout.

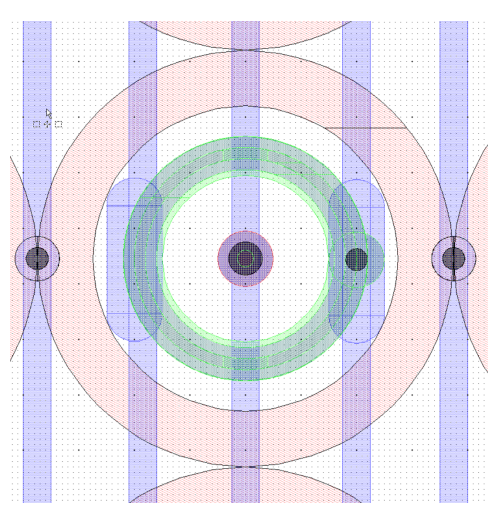


Figure A.4: MIC_ARRAY_1_L layout.

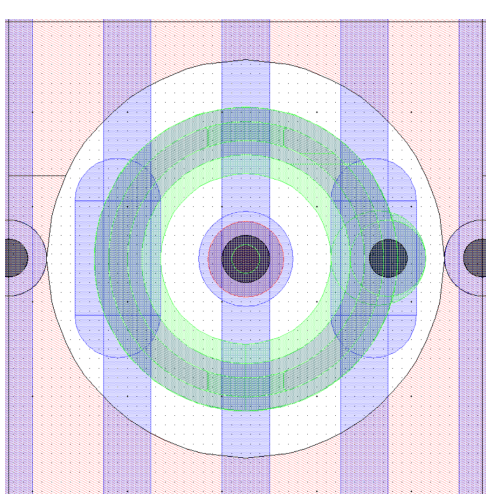


Figure A.5: MIC_ARRAY_2 layout.

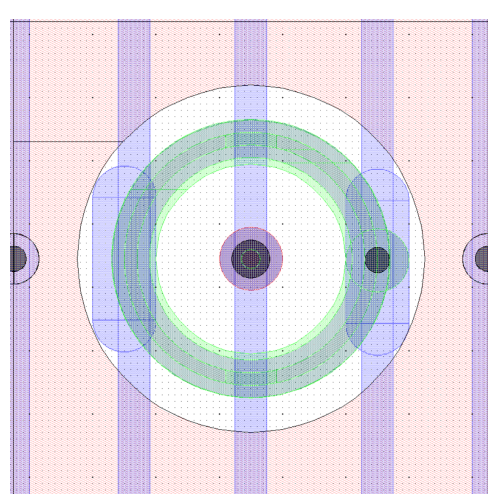


Figure A.6: MIC_ARRAY_2_L layout.

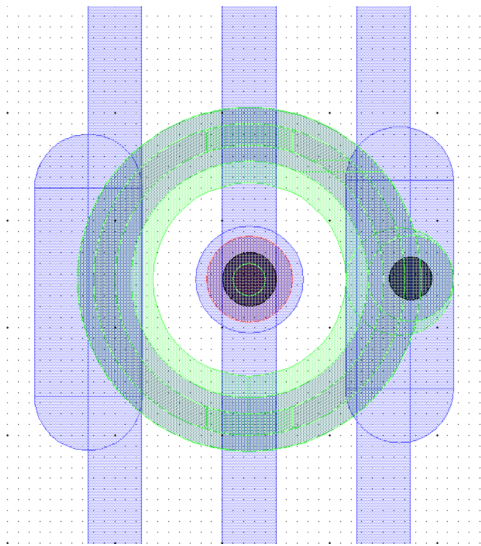


Figure A.7: MIC_ARRAY_3 layout.

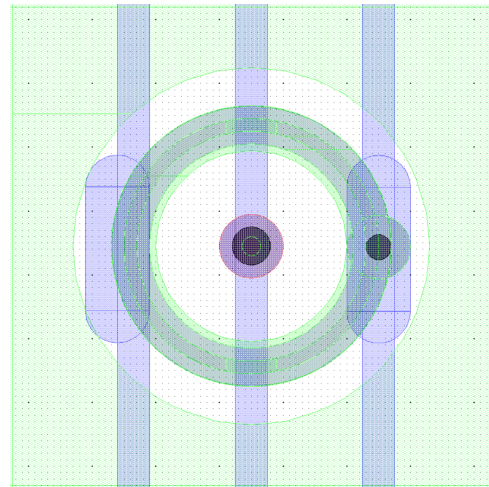


Figure A.8: MIC_ARRAY_3_L layout.

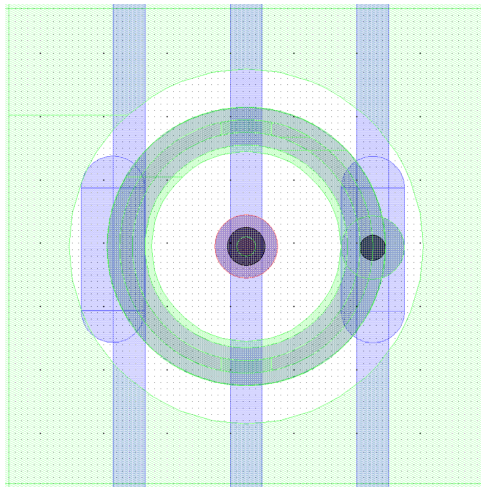


Figure A.9: MIC_ARRAY_3_PSTOP_L layout-out.

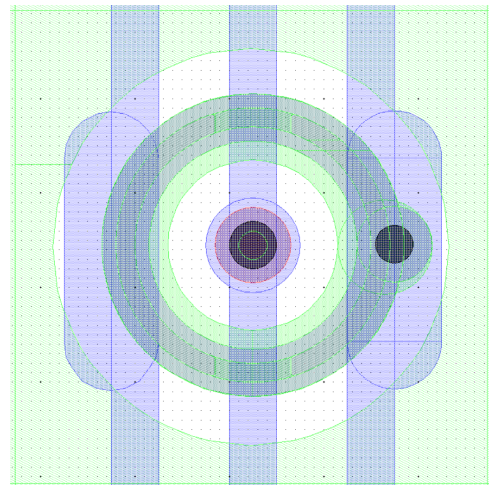


Figure A.10: MIC_ARRAY_PSTOP layout.

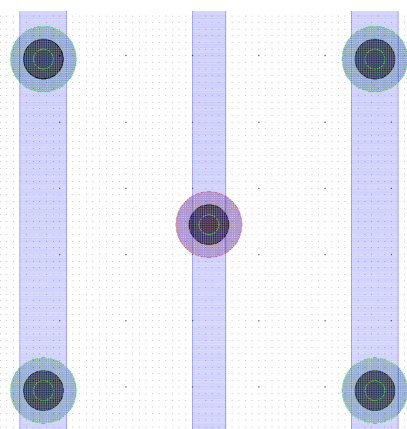


Figure A.11: MIC_3D layout. Every second column is n+ or p+ pillars.

Appendix B: Detector Interface PCB

A PCB was needed to connect the detector to the outside world, as the detector pads are too small for any other connection than wire-bonding. This PCB could simply have consisted of wire-bonding pads going to connectors for cables, but it was decided to make a more multi-purpose board to make it simple to try different set-ups. The board was made so that it is possible to connect the substrate, the guard rings, and the p+ rings individually to ground or external bias. It is also possible to read out the guard rings of the cells. Each channel can also be connected to a bias filter for removal of high frequency noise. The n+ core readout channel was designed to add as little capacitance as possible. LEMO connectors were chosen to connect to the outside world as they are well shielded and much used at IFT. The exposed metal is coated with electroless nickel immersion gold (ENIG) to provide better contact for wire-bonding. One mistake was done with the PCB design in that solder mask where the detector is mounted was forgotten. This has no consequences for the 3DMiMic detector, since there is an insulating layer between the bulk and the support wafer. The solder resist can be scratched off if the PCB is to be used for a different detector. The layout of the PCB can be seen in figure B.2 and a photograph can be seen in figure B.1.

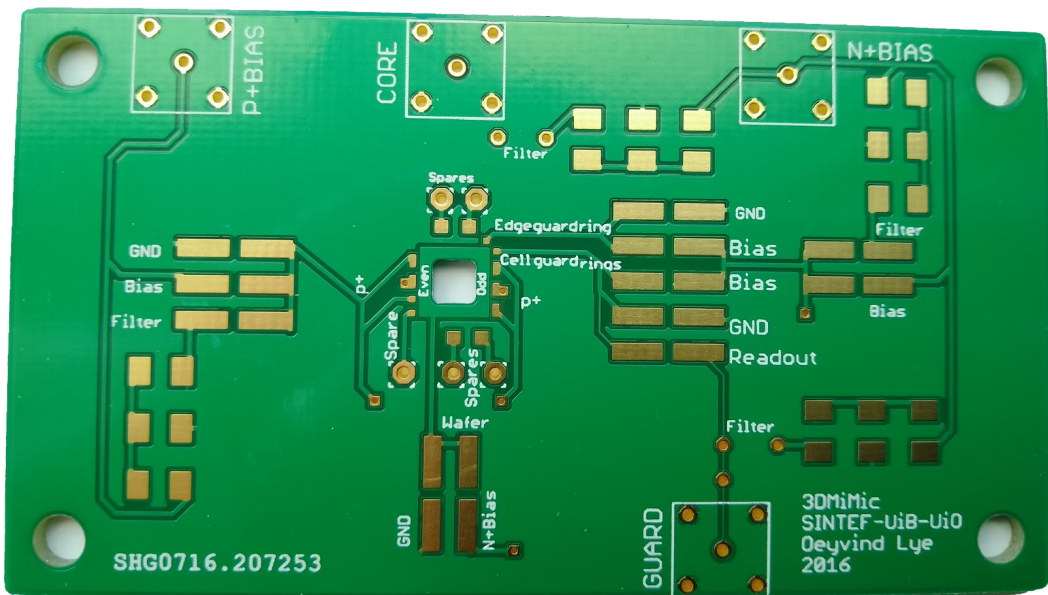


Figure B.1: Top side of PCB.

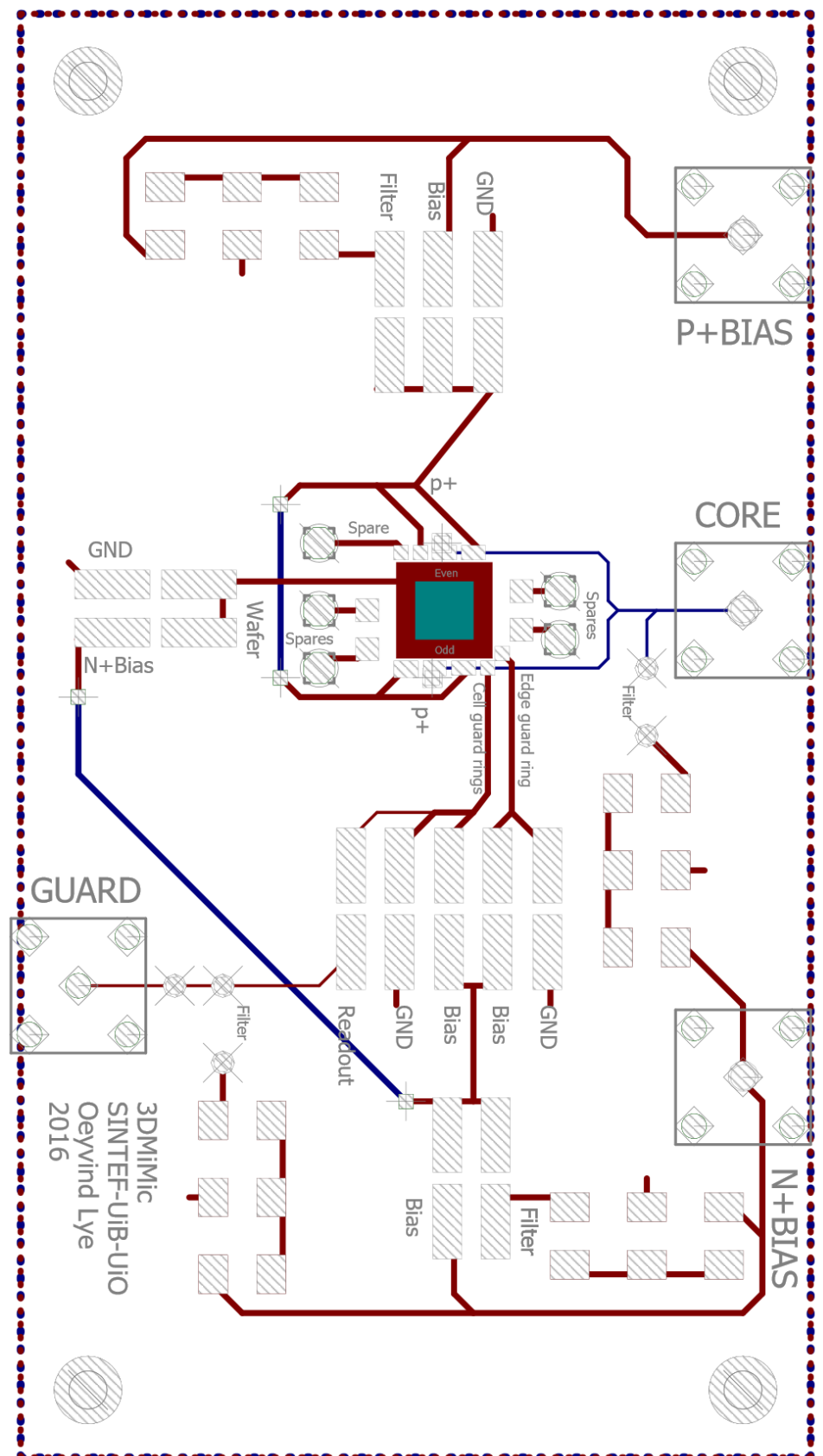


Figure B.2: PCB layout. Ground planes not shown.

After the design had been produced, it was again considered to read out the two sides of the detector separately, instead of in one signal. On the PCB, this can be solved by wire-bonding one of the sides to one of the spare pads and connecting this to the through-hole by the GUARD connector with a wire. To avoid extra capacitance, the wires leading to the unused surface-mounting pads can be cut with a knife.